Fermilab-Pub-10-333-E

Measurement of $t\bar{t}$ production in the tau + jets channel using $p\bar{p}$ collisions at $\sqrt{s} = 1.96$ TeV

V.M. Abazov,[35] B. Abbott,[73] M. Abolins,[62] B.S. Acharya,[29] M. Adams,[48] T. Adams,[46] G.D. Alexeev,[35] G. Alkhazov,[39] A. Alton[a],[61] G. Alverson,[60] G.A. Alves,[2] L.S. Ancu,[34] M. Aoki,[47] Y. Arnoud,[14] M. Arov,[57] A. Askew,[46] B. Åsman,[40] O. Atramentov,[65] C. Avila,[8] J. BackusMayes,[80] F. Badaud,[13] L. Bagby,[47] B. Baldin,[47] D.V. Bandurin,[46] S. Banerjee,[29] E. Barberis,[60] P. Baringer,[55] J. Barreto,[2] J.F. Bartlett,[47] U. Bassler,[18] V. Bazterra,[48] S. Beale,[6] A. Bean,[55] M. Begalli,[3] M. Begel,[71] C. Belanger-Champagne,[40] L. Bellantoni,[47] S.B. Beri,[27] G. Bernardi,[17] R. Bernhard,[22] I. Bertram,[41] M. Besançon,[18] R. Beuselinck,[42] V.A. Bezzubov,[38] P.C. Bhat,[47] V. Bhatnagar,[27] G. Blazey,[49] S. Blessing,[46] K. Bloom,[64] A. Boehnlein,[47] D. Boline,[70] T.A. Bolton,[56] E.E. Boos,[37] G. Borissov,[41] T. Bose,[59] A. Brandt,[76] O. Brandt,[23] R. Brock,[62] G. Brooijmans,[68] A. Bross,[47] D. Brown,[17] J. Brown,[17] X.B. Bu,[7] D. Buchholz,[50] M. Buehler,[79] V. Buescher,[24] V. Bunichev,[37] S. Burdin[b],[41] T.H. Burnett,[80] C.P. Buszello,[42] B. Calpas,[15] E. Camacho-Pérez,[32] M.A. Carrasco-Lizarraga,[32] B.C.K. Casey,[47] H. Castilla-Valdez,[32] S. Chakrabarti,[70] D. Chakraborty,[49] K.M. Chan,[53] A. Chandra,[78] G. Chen,[55] S. Chevalier-Théry,[18] D.K. Cho,[75] S.W. Cho,[31] S. Choi,[31] B. Choudhary,[28] T. Christoudias,[42] S. Cihangir,[47] D. Claes,[64] J. Clutter,[55] M. Cooke,[47] W.E. Cooper,[47] M. Corcoran,[78] F. Couderc,[18] M.-C. Cousinou,[15] A. Croc,[18] D. Cutts,[75] M. Ćwiok,[30] A. Das,[44] G. Davies,[42] K. De,[76] S.J. de Jong,[34] E. De La Cruz-Burelo,[32] F. Déliot,[18] M. Demarteau,[47] R. Demina,[69] D. Denisov,[47] S.P. Denisov,[38] S. Desai,[47] K. DeVaughan,[64] H.T. Diehl,[47] M. Diesburg,[47] A. Dominguez,[64] T. Dorland,[80] A. Dubey,[28] L.V. Dudko,[37] D. Duggan,[65] A. Duperrin,[15] S. Dutt,[27] A. Dyshkant,[49] M. Eads,[64] D. Edmunds,[62] J. Ellison,[45] V.D. Elvira,[47] Y. Enari,[17] S. Eno,[58] H. Evans,[51] A. Evdokimov,[71] V.N. Evdokimov,[38] G. Facini,[60] T. Ferbel,[58,69] F. Fiedler,[24] F. Filthaut,[34] W. Fisher,[62] H.E. Fisk,[47] M. Fortner,[49] H. Fox,[41] S. Fuess,[47] T. Gadfort,[71] A. Garcia-Bellido,[69] V. Gavrilov,[36] P. Gay,[13] W. Geist,[19] W. Geng,[15,62] D. Gerbaudo,[66] C.E. Gerber,[48] Y. Gershtein,[65] G. Ginther,[47,69] G. Golovanov,[35] A. Goussiou,[80] P.D. Grannis,[70] S. Greder,[19] H. Greenlee,[47] Z.D. Greenwood,[57] E.M. Gregores,[4] G. Grenier,[20] Ph. Gris,[13] J.-F. Grivaz,[16] A. Grohsjean,[18] S. Grünendahl,[47] M.W. Grünewald,[30] F. Guo,[70] J. Guo,[70] G. Gutierrez,[47] P. Gutierrez,[73] A. Haas[c],[68] S. Hagopian,[46] J. Haley,[60] L. Han,[7] K. Harder,[43] A. Harel,[69] J.M. Hauptman,[54] J. Hays,[42] T. Head,[43] T. Hebbeker,[21] D. Hedin,[49] H. Hegab,[74] A.P. Heinson,[45] U. Heintz,[75] C. Hensel,[23] I. Heredia-De La Cruz,[32] K. Herner,[61] G. Hesketh,[60] M.D. Hildreth,[53] R. Hirosky,[79] T. Hoang,[46] J.D. Hobbs,[70] B. Hoeneisen,[12] M. Hohlfeld,[24] S. Hossain,[73] Z. Hubacek,[10] N. Huske,[17] V. Hynek,[10] I. Iashvili,[67] R. Illingworth,[47] A.S. Ito,[47] S. Jabeen,[75] M. Jaffré,[16] S. Jain,[67] D. Jamin,[15] R. Jesik,[42] K. Johns,[44] M. Johnson,[47] D. Johnston,[64] A. Jonckheere,[47] P. Jonsson,[42] J. Joshi,[27] A. Juste[d],[47] K. Kaadze,[56] E. Kajfasz,[15] D. Karmanov,[37] P.A. Kasper,[47] I. Katsanos,[64] R. Kehoe,[77] S. Kermiche,[15] N. Khalatyan,[47] A. Khanov,[74] A. Kharchilava,[67] Y.N. Kharzheev,[35] D. Khatidze,[75] M.H. Kirby,[50] J.M. Kohli,[27] A.V. Kozelov,[38] J. Kraus,[62] A. Kumar,[67] A. Kupco,[11] T. Kurča,[20] V.A. Kuzmin,[37] J. Kvita,[9] S. Lammers,[51] G. Landsberg,[75] P. Lebrun,[20] H.S. Lee,[31] S.W. Lee,[54] W.M. Lee,[47] J. Lellouch,[17] L. Li,[45] Q.Z. Li,[47] S.M. Lietti,[5] J.K. Lim,[31] D. Lincoln,[47] J. Linnemann,[62] V.V. Lipaev,[38] R. Lipton,[47] Y. Liu,[7] Z. Liu,[6] A. Lobodenko,[39] M. Lokajicek,[11] P. Love,[41] H.J. Lubatti,[80] R. Luna-Garcia[e],[32] A.L. Lyon,[47] A.K.A. Maciel,[2] D. Mackin,[78] R. Madar,[18] R. Magaña-Villalba,[32] S. Malik,[64] V.L. Malyshev,[35] Y. Maravin,[56] J. Martínez-Ortega,[32] R. McCarthy,[70] C.L. McGivern,[55] M.M. Meijer,[34] A. Melnitchouk,[63] D. Menezes,[49] P.G. Mercadante,[4] M. Merkin,[37] A. Meyer,[21] J. Meyer,[23] N.K. Mondal,[29] G.S. Muanza,[15] M. Mulhearn,[79] E. Nagy,[15] M. Naimuddin,[28] M. Narain,[75] R. Nayyar,[28] H.A. Neal,[61] J.P. Negret,[8] P. Neustroev,[39] S.F. Novaes,[5] T. Nunnemann,[25] G. Obrant,[39] J. Orduna,[32] N. Osman,[42] J. Osta,[53] G.J. Otero y Garzón,[1] M. Owen,[43] M. Padilla,[45] M. Pangilinan,[75] N. Parashar,[52] V. Parihar,[75] S.K. Park,[31] J. Parsons,[68] R. Partridge[c],[75] N. Parua,[51] A. Patwa,[71] B. Penning,[47] M. Perfilov,[37] K. Peters,[43] Y. Peters,[43] G. Petrillo,[69] P. Pétroff,[16] R. Piegaia,[1] J. Piper,[62] M.-A. Pleier,[71] P.L.M. Podesta-Lerma[f],[32] V.M. Podstavkov,[47] M.-E. Pol,[2] P. Polozov,[36] A.V. Popov,[38] M. Prewitt,[78] D. Price,[51] S. Protopopescu,[71] J. Qian,[61] A. Quadt,[23] B. Quinn,[63] M.S. Rangel,[2] K. Ranjan,[28] P.N. Ratoff,[41] I. Razumov,[38] P. Renkel,[77] P. Rich,[43] M. Rijssenbeek,[70] I. Ripp-Baudot,[19] F. Rizatdinova,[74] M. Rominsky,[47] C. Royon,[18] P. Rubinov,[47] R. Ruchti,[53] G. Safronov,[36] G. Sajot,[14] A. Sánchez-Hernández,[32] M.P. Sanders,[25] B. Sanghi,[47] A.S. Santos,[5]

G. Savage,[47] L. Sawyer,[57] T. Scanlon,[42] R.D. Schamberger,[70] Y. Scheglov,[39] H. Schellman,[50] T. Schliephake,[26] S. Schlobohm,[80] C. Schwanenberger,[43] R. Schwienhorst,[62] J. Sekaric,[55] H. Severini,[73] E. Shabalina,[23] V. Shary,[18] A.A. Shchukin,[38] R.K. Shivpuri,[28] V. Simak,[10] V. Sirotenko,[47] P. Skubic,[73] P. Slattery,[69] D. Smirnov,[53] K.J. Smith,[67] G.R. Snow,[64] J. Snow,[72] S. Snyder,[71] S. Söldner-Rembold,[43] L. Sonnenschein,[21] A. Sopczak,[41] M. Sosebee,[76] K. Soustruznik,[9] B. Spurlock,[76] J. Stark,[14] V. Stolin,[36] D.A. Stoyanova,[38] E. Strauss,[70] M. Strauss,[73] D. Strom,[48] L. Stutte,[47] P. Svoisky,[73] M. Takahashi,[43] A. Tanasijczuk,[1] W. Taylor,[6] M. Titov,[18] V.V. Tokmenin,[35] D. Tsybychev,[70] B. Tuchming,[18] C. Tully,[66] P.M. Tuts,[68] L. Uvarov,[39] S. Uvarov,[39] S. Uzunyan,[49] R. Van Kooten,[51] W.M. van Leeuwen,[33] N. Varelas,[48] E.W. Varnes,[44] I.A. Vasilyev,[38] P. Verdier,[20] L.S. Vertogradov,[35] M. Verzocchi,[47] M. Vesterinen,[43] D. Vilanova,[18] P. Vint,[42] P. Vokac,[10] H.D. Wahl,[46] M.H.L.S. Wang,[69] J. Warchol,[53] G. Watts,[80] M. Wayne,[53] M. Weber[g],[47] L. Welty-Rieger,[50] M. Wetstein,[58] A. White,[76] D. Wicke,[24] M.R.J. Williams,[41] G.W. Wilson,[55] S.J. Wimpenny,[45] M. Wobisch,[57] D.R. Wood,[60] T.R. Wyatt,[43] Y. Xie,[47] C. Xu,[61] S. Yacoob,[50] R. Yamada,[47] W.-C. Yang,[43] T. Yasuda,[47] Y.A. Yatsunenko,[35] Z. Ye,[47] H. Yin,[7] K. Yip,[71] H.D. Yoo,[75] S.W. Youn,[47] J. Yu,[76] S. Zelitch,[79] T. Zhao,[80] B. Zhou,[61] J. Zhu,[61] M. Zielinski,[69] D. Zieminska,[51] and L. Zivkovic[68]

(The D0 Collaboration*)

[1] *Universidad de Buenos Aires, Buenos Aires, Argentina*
[2] *LAFEX, Centro Brasileiro de Pesquisas Físicas, Rio de Janeiro, Brazil*
[3] *Universidade do Estado do Rio de Janeiro, Rio de Janeiro, Brazil*
[4] *Universidade Federal do ABC, Santo André, Brazil*
[5] *Instituto de Física Teórica, Universidade Estadual Paulista, São Paulo, Brazil*
[6] *Simon Fraser University, Vancouver, British Columbia, and York University, Toronto, Ontario, Canada*
[7] *University of Science and Technology of China, Hefei, People's Republic of China*
[8] *Universidad de los Andes, Bogotá, Colombia*
[9] *Charles University, Faculty of Mathematics and Physics, Center for Particle Physics, Prague, Czech Republic*
[10] *Czech Technical University in Prague, Prague, Czech Republic*
[11] *Center for Particle Physics, Institute of Physics, Academy of Sciences of the Czech Republic, Prague, Czech Republic*
[12] *Universidad San Francisco de Quito, Quito, Ecuador*
[13] *LPC, Université Blaise Pascal, CNRS/IN2P3, Clermont, France*
[14] *LPSC, Université Joseph Fourier Grenoble 1, CNRS/IN2P3, Institut National Polytechnique de Grenoble, Grenoble, France*
[15] *CPPM, Aix-Marseille Université, CNRS/IN2P3, Marseille, France*
[16] *LAL, Université Paris-Sud, CNRS/IN2P3, Orsay, France*
[17] *LPNHE, Universités Paris VI and VII, CNRS/IN2P3, Paris, France*
[18] *CEA, Irfu, SPP, Saclay, France*
[19] *IPHC, Université de Strasbourg, CNRS/IN2P3, Strasbourg, France*
[20] *IPNL, Université Lyon 1, CNRS/IN2P3, Villeurbanne, France and Université de Lyon, Lyon, France*
[21] *III. Physikalisches Institut A, RWTH Aachen University, Aachen, Germany*
[22] *Physikalisches Institut, Universität Freiburg, Freiburg, Germany*
[23] *II. Physikalisches Institut, Georg-August-Universität Göttingen, Göttingen, Germany*
[24] *Institut für Physik, Universität Mainz, Mainz, Germany*
[25] *Ludwig-Maximilians-Universität München, München, Germany*
[26] *Fachbereich Physik, Bergische Universität Wuppertal, Wuppertal, Germany*
[27] *Panjab University, Chandigarh, India*
[28] *Delhi University, Delhi, India*
[29] *Tata Institute of Fundamental Research, Mumbai, India*
[30] *University College Dublin, Dublin, Ireland*
[31] *Korea Detector Laboratory, Korea University, Seoul, Korea*
[32] *CINVESTAV, Mexico City, Mexico*
[33] *FOM-Institute NIKHEF and University of Amsterdam/NIKHEF, Amsterdam, The Netherlands*
[34] *Radboud University Nijmegen/NIKHEF, Nijmegen, The Netherlands*
[35] *Joint Institute for Nuclear Research, Dubna, Russia*
[36] *Institute for Theoretical and Experimental Physics, Moscow, Russia*
[37] *Moscow State University, Moscow, Russia*
[38] *Institute for High Energy Physics, Protvino, Russia*
[39] *Petersburg Nuclear Physics Institute, St. Petersburg, Russia*
[40] *Stockholm University, Stockholm and Uppsala University, Uppsala, Sweden*
[41] *Lancaster University, Lancaster LA1 4YB, United Kingdom*
[42] *Imperial College London, London SW7 2AZ, United Kingdom*
[43] *The University of Manchester, Manchester M13 9PL, United Kingdom*

[44] University of Arizona, Tucson, Arizona 85721, USA
[45] University of California Riverside, Riverside, California 92521, USA
[46] Florida State University, Tallahassee, Florida 32306, USA
[47] Fermi National Accelerator Laboratory, Batavia, Illinois 60510, USA
[48] University of Illinois at Chicago, Chicago, Illinois 60607, USA
[49] Northern Illinois University, DeKalb, Illinois 60115, USA
[50] Northwestern University, Evanston, Illinois 60208, USA
[51] Indiana University, Bloomington, Indiana 47405, USA
[52] Purdue University Calumet, Hammond, Indiana 46323, USA
[53] University of Notre Dame, Notre Dame, Indiana 46556, USA
[54] Iowa State University, Ames, Iowa 50011, USA
[55] University of Kansas, Lawrence, Kansas 66045, USA
[56] Kansas State University, Manhattan, Kansas 66506, USA
[57] Louisiana Tech University, Ruston, Louisiana 71272, USA
[58] University of Maryland, College Park, Maryland 20742, USA
[59] Boston University, Boston, Massachusetts 02215, USA
[60] Northeastern University, Boston, Massachusetts 02115, USA
[61] University of Michigan, Ann Arbor, Michigan 48109, USA
[62] Michigan State University, East Lansing, Michigan 48824, USA
[63] University of Mississippi, University, Mississippi 38677, USA
[64] University of Nebraska, Lincoln, Nebraska 68588, USA
[65] Rutgers University, Piscataway, New Jersey 08855, USA
[66] Princeton University, Princeton, New Jersey 08544, USA
[67] State University of New York, Buffalo, New York 14260, USA
[68] Columbia University, New York, New York 10027, USA
[69] University of Rochester, Rochester, New York 14627, USA
[70] State University of New York, Stony Brook, New York 11794, USA
[71] Brookhaven National Laboratory, Upton, New York 11973, USA
[72] Langston University, Langston, Oklahoma 73050, USA
[73] University of Oklahoma, Norman, Oklahoma 73019, USA
[74] Oklahoma State University, Stillwater, Oklahoma 74078, USA
[75] Brown University, Providence, Rhode Island 02912, USA
[76] University of Texas, Arlington, Texas 76019, USA
[77] Southern Methodist University, Dallas, Texas 75275, USA
[78] Rice University, Houston, Texas 77005, USA
[79] University of Virginia, Charlottesville, Virginia 22901, USA
[80] University of Washington, Seattle, Washington 98195, USA

(Dated: August 24, 2010)

We present a measurement of the $t\bar{t}$ production cross section multiplied by the branching ratio to tau lepton decaying semi-hadronically (τ_h) plus jets, $\sigma(p\bar{p} \to t\bar{t}+X) \cdot \mathrm{BR}(t\bar{t} \to \tau_h + \mathrm{jets})$, at a center of mass energy $\sqrt{s} = 1.96$ TeV using 1 fb^{-1} of integrated luminosity collected with the D0 detector. Assuming a top quark mass of 170 GeV, we measure $\sigma_{t\bar{t}} \cdot \mathrm{BR}_{\tau_h+j} = 0.60^{+0.23}_{-0.22}$ (stat) $^{+0.15}_{-0.14}$ (syst) $\pm$ 0.04 (lum) pb. In addition, we extract the $t\bar{t}$ production cross section using the $t\bar{t} \to \tau_h +$ jets topology, with the result $\sigma_{t\bar{t}} = 6.9\ ^{+1.2}_{-1.2}$ (stat) $^{+0.8}_{-0.7}$ (syst) ± 0.4 (lum) pb. These findings are in good agreement with standard model predictions and measurements performed using other top quark decay channels.

PACS numbers: 13.85.Lg, 13.85.Ni, 13.85.Qk, 14.65.Ha

The decay $t \to Wb \to \tau\nu_\tau b$ provides a unique laboratory in which to investigate the properties of the third generation fermions — the top (t) and bottom (b) quarks, the tau lepton (τ), and the tau neutrino (ν_τ) — in a single process. In the standard model (SM), the t quark branching ratio (BR) to a W boson and a b quark is $\approx 100\%$, and the final state is determined by the SM BR of the W boson. Since the t is the heaviest quark and the τ the heaviest lepton, any non-SM mass- or flavor-dependent couplings could change the t quark decay rate into final states with τ leptons. Therefore, any deviation in the BR of $t \to \tau\nu_\tau b$ from that predicted by the SM can be an indication of non-SM physics. For example, in the Type 2 two-Higgs doublet model [1], such as required by the minimal supersymmetric standard model [2], the t quark can have a significant BR to a charged Higgs bo-

*with visitors from [a]Augustana College, Sioux Falls, SD, USA, [b]The University of Liverpool, Liverpool, UK, [c]SLAC, Menlo Park, CA, USA, [d]ICREA/IFAE, Barcelona, Spain, [e]Centro de Investigacion en Computacion - IPN, Mexico City, Mexico, [f]ECFM, Universidad Autonoma de Sinaloa, Culiacán, Mexico, and [g]Universität Bern, Bern, Switzerland.

son ($H^{\pm}$) and a b quark if $m_{H^{\pm}} < m_t - m_b$. For large values of $\tan\beta$, the ratio of the vacuum expectation values of the two Higgs doublets, the charged Higgs boson preferentially decays to $\tau\nu_\tau$, thereby increasing the BR of $t \to \tau\nu_\tau b$ relative to the SM expectation and leading to a larger measured $\sigma(p\bar{p} \to t\bar{t} + X) \cdot \mathrm{BR}(t\bar{t} \to \tau + \mathrm{jets})$ compared to the value expected from SM assumptions for the BRs and the production cross section [3–5]. Other possible non-SM processes that can enhance the t quark to τ lepton BR are R-parity violating decays of the t quark in supersymetric models [6] and new Z' bosons with non-universal couplings [7].

In this article, we present the first measurement of $t\bar{t}$ production in the $\tau +$ jets final state using a data sample corresponding to an integrated luminosity of 1 fb^{-1} collected with the D0 detector [8] at the Fermilab Tevatron $p\bar{p}$ Collider operating at a center of mass energy $\sqrt{s} = 1.96$ TeV. This measurement uses semi-hadronic τ lepton decays, with BR $\approx 65\%$, as secondary electrons and muons from τ lepton decays are difficult to distinguish from primary electrons and muons resulting from W decays. Previous measurements of $t\bar{t}$ production using τ leptons in the final state have been performed by the D0 [9] and CDF [10] collaborations in the $\tau_h + \ell$ channel, where τ_h represents semi-hadronic τ lepton decay modes and ℓ represents either an electron or a muon.

We apply the following preselection requirements: events must satisfy a multijet trigger requiring at least four jets; this is the same trigger used in the $t\bar{t}$ cross section measurement in the all-hadronic decay mode [11]. Reconstructed events are required to have missing transverse energy $\not\!\!E_T \geq 15$ GeV and $\not\!\!E_T$ significance > 3, where the $\not\!\!E_T$ significance is a measure of the likelihood that the $\not\!\!E_T$ arises from physical sources rather than fluctuations in the measurement of the energies of the physics objects (jets, muons, electrons and unclustered energy) [12]. Each event must also have at least four reconstructed jets with pseudorapidity $|\eta| < 2.5$ and transverse momentum $p_T > 15$ GeV using an iterative jet cone algorithm [13] with a cone size $\Delta\mathcal{R} = \sqrt{(\Delta\eta)^2 + (\Delta\phi)^2} = 0.5$ [14]. The jet energies are corrected for the energy response of the calorimeter, the cone size, multiple $p\bar{p}$ interactions, event pile-up, and calorimeter noise [15]. At least one jet is required to have $p_T > 35$ GeV, and at least two jets are required to have $p_T > 25$ GeV. Each event is also required to have at least one τ_h candidate with $p_T > 10$ GeV, $|\eta| < 2.5$, and tau neural network output, $NN_\tau > 0.3$ [16]. Finally, to ensure this analysis is statistically independent of other D0 $t\bar{t}$ cross section measurements so that it can be included in a combined cross section measurement, events satisfying the requirements of the $t\bar{t} \to e(\mu) +$ jets channel [17], which include an isolated electron (muon) with $p_T > 20$ GeV, are rejected, as are events satisfying the requirements of the $t\bar{t}$ cross section measurement in the all-hadronic channel [11].

A semi-hadronic τ lepton candidate is a calorimeter cluster of cone size $\Delta\mathcal{R} = 0.5$ that includes any subclusters that might be present with $E > 800$ MeV constructed from cells in the electromagnetic (EM) section of the calorimeter and the associated tracks with $p_T > 1.5$ GeV in a cone $\Delta\mathcal{R} = 0.3$ contained within the calorimeter cluster. These τ candidates are classified according to one of three types based on the number of tracks and activity in the EM calorimeter, motivated by the semi-hadronic τ lepton decays: (1) $\tau^{\pm} \to \pi^{\pm}\nu_\tau$, (2) $\tau^{\pm} \to \pi^{\pm}\pi^0\nu_\tau$, (3) $\tau^{\pm} \to \pi^{\pm}\pi^{\pm}\pi^{\mp}(\pi^0)\nu_\tau$. We define the three tau-types as follows: a single track with no EM sub-clusters (tau-type 1); a single track and ≥ 1 EM subclusters (tau-type 2); and at least two tracks and ≥ 0 EM sub-clusters (tau-type 3).

To further reduce the number of quark and gluon jets reconstructed as τ leptons, we train separate neural networks for each semi-hadronic τ lepton decay type to improve the discrimination of τ lepton candidates from the jet background. The input variables to NN_τ are chosen to be minimally dependent on the τ lepton energy and to exploit the low track multiplicity and the narrow width of the calorimeter cluster produced by τ leptons decaying semi-hadronically, the low mass of the τ lepton, and the differences in longitudinal and transverse shower shapes between τ leptons and jets [16]. Each NN_τ is trained on $Z \to \tau^+\tau^-$ Monte Carlo (MC) events for signal and jets from data, where a jet and a non-isolated muon are back-to-back in ϕ, for background.

To measure the number of $t\bar{t} \to \tau_h +$jets signal events in data, the physics and instrumental backgrounds must be determined. The main physics backgrounds are $W +$ jets events, where the W boson decays to a τ lepton, and to a smaller extent $Z +$ jets events, where the Z boson decays to a pair of τ leptons with one misidentified as a jet and the $\not\!\!E_T$ is due to the neutrinos from the decays of the τ leptons. The main instrumental background is multijet production where a jet is misidentified as a τ lepton and the energy is mismeasured leading to a net $\not\!\!E_T$.

The preselection efficiencies and SM BRs for $t\bar{t}$ to final states with leptons [18] are given in Table I. These, as well as the final efficiencies, are calculated using a MC simulation of the experiment. The $t\bar{t}$ signal with leptons in the final state and $W(Z) +$ jets background are simulated using the ALPGEN 1.2 [19] matrix element generator assuming a t quark mass of 170 GeV and using the CTEQ6L1 [20] parton distribution function (PDF) set. These events are then processed through PYTHIA 6.2 [21] to simulate parton showering, fragmentation, hadronization, and decays of short lived particles, except for b hadrons and τ leptons. EVTGEN [22] is used to model the decays of b hadrons, while τ leptons are decayed using TAUOLA [23]. To avoid double counting final states generated by the leading-order parton-level calculation of ALPGEN and the parton-level shower evolution of PYTHIA, a matching algorithm is used [24]. The

TABLE I: A summary of the SM BRs of the various $t\bar{t}$ subprocesses and the preselection efficiencies, where the uncertainties are derived from MC statistics. The leptonic τ lepton decays are included in the e and μ channels, and $l^{\pm}$ represents an e, μ or τ lepton.

	BR (%)	$\epsilon_{\text{preselection}}$ (%)
$t\bar{t} \to \tau_h + \text{jets}$	9.75	42.1±0.2
$t\bar{t} \to e + \text{jets}$	17.7	17.5±0.2
$t\bar{t} \to \mu + \text{jets}$	17.6	11.5±0.1
$t\bar{t} \to l^+l^- + \text{jets}$	11.1	4.16±0.03

generated events are then processed through the GEANT-based [25] simulation of the D0 detector providing tracking hits, calorimeter cell energies and muon hit information. The same reconstruction algorithm is applied to data and simulated events.

The preselected data sample is used to extract the signal and to study the multijet background after additional selection criteria are applied. To extract the signal sample, we require $NN_\tau > 0.95$. The selected events are then separated on the basis of tau-type according to the τ lepton candidate with the highest value of NN_τ. This is done primarily to separate tau-type 3 events from the tau-type 1 and 2 events, since the former has a much higher misidentification rate and thus results in larger uncertainties on the $t\bar{t}$ cross section. In addition, we require that each event have at least one identified b jet using the b-tag neural network (NN_b) with the requirement $NN_b > 0.775$. The NN_b uses nine input variables that characterize the presence and properties of secondary vertices and track impact parameters within the jet [26]. The efficiencies of these selections are shown in Table II.

The expected fraction of $t\bar{t}$ events in the signal sample is $\approx 15\%$ for tau-type 1 and 2, and $\approx 3\%$ for tau-type 3 assuming $\sigma_{t\bar{t}} = 6.9$ pb as measured in this analysis. In addition, the signal sample contains $W(Z) + \text{jets}$ and multijet background events that must be subtracted. The $W(Z) + \text{jets}$ contamination is determined using MC events, while the multijet background is determined from data. We start with the preselected sample and apply a loose τ lepton veto, $NN_\tau < 0.9$. Using MC events, we expect that the resulting sample contains $< 2\%$ $t\bar{t} \to \tau_h + \text{jets}$ events and $< 3\%$ $W(Z) + \text{jets}$ events, and therefore provides a good representation of the multijet background. To further improve the modeling, the $W(Z) + \text{jets}$ expectation is subtracted from the multijet background data sample.

The numbers of signal and background events are extracted from the final selected sample using a neural network (NN_{sb}) event discriminant with the following input variables: (1) the scalar sum of the p_T of all jets and the τ lepton candidate in the event; (2) the aplanarity [27]; (3) the $\not\!\!E_T$ significance; (4) the invariant mass of all jets and the τ lepton candidate in the event; and (5) a χ^2 representing how well the 2 and 3 jet invariant masses agree with values expected for hadronic t quark decays, $\chi^2 = (M_{3\text{jet}} - m_t)/\sigma_t^2 + (M_{2\text{jet}} - m_W)^2/\sigma_W^2$, with $M_{2\text{jet}}$ ($M_{3\text{jet}}$) being the 2 (3) jet invariant mass, $m_t = 170$ GeV, $\sigma_t = 45$ GeV and $m_W = 80$ GeV, $\sigma_W = 10$ GeV are the mass and its resolution in the all-hadronic final state for the t quark and W boson, respectively. The jet combination minimizing the χ^2 is used. The NN_{sb} is trained using a generated $t\bar{t} \to \tau_h + \text{jets}$ MC sample for signal and half the multijet data sample for background.

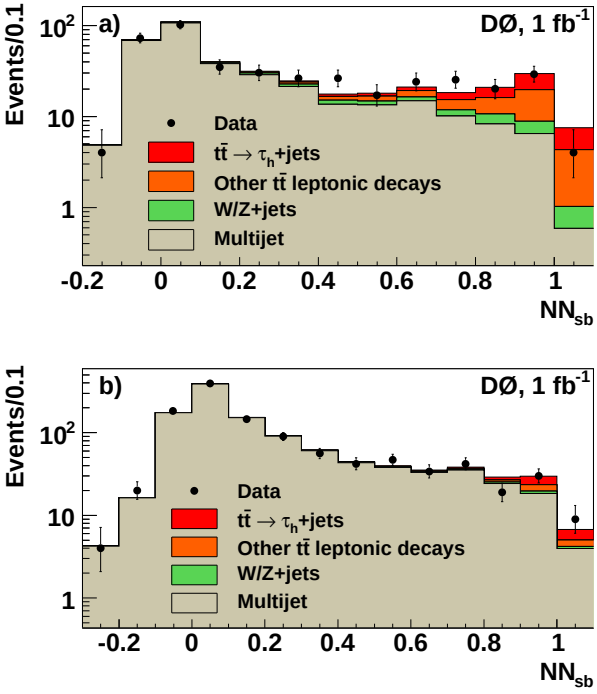

FIG. 1: The output of NN_{sb} for a) the tau-type 1 and 2 channel, b) the tau-type 3 channel. The χ^2 per degree of freedom between data and templates is 0.6 for a) and 0.5 for b).

We apply the trained NN_{sb} to the signal data sample, the remaining half of the multijet sample, a $t\bar{t}$ MC sample with leptons in the final state that is independent of the NN_{sb} training sample, and a $W(Z) + \text{jets}$ MC sample. The application of NN_{sb} on the multijet and MC samples is used to generate templates, as shown in Fig. 1, that are used to determine the fraction of $t\bar{t}$ and multijet events using a negative log-likelihood fit. The normalization of the $W(Z) + \text{jets}$ MC sample is derived by scaling the $W(Z)$ transverse (dilepton) mass distribution to data. The normalization for $t\bar{t} \to e(\mu) + \text{jets}$ is fixed to the theoretical cross section [5] and BRs.

The number of $t\bar{t} \to \tau_h + \text{jets}$ events extracted from the fit to data are $25.1^{+11.2}_{-10.5}$ (stat) and $18.0^{+11.3}_{-10.5}$ (stat) for channels with tau-types 1 and 2 together, and with tau-type 3, respectively. The fitted numbers of the multijet background events are $336.4^{+11.2}_{-10.5}$ (stat) and

TABLE II: The efficiencies for the tight τ lepton candidate ($NN_\tau > 0.95$) and b-tagging selections for tau-type 1 and 2, and tau-type 3 channels. The uncertainties are based on MC statistics.

	tau types 1 and 2 $NN_\tau > 0.95$ (%)	tau types 1 and 2 b-tag (%)	tau type 3 $NN_\tau > 0.95$ (%)	tau type 3 b-tag (%)
$t\bar{t} \to \tau_h + \text{jets}$	23.7±0.3	$60.1\ ^{+2.8}_{-2.7}$	19.4±0.2	$59.9\ ^{+2.8}_{-2.7}$
$t\bar{t} \to e + \text{jets}$	33.1±0.4	$58.7\ ^{+2.8}_{-2.7}$	8.1±0.2	$58.9\ ^{+2.8}_{-2.7}$
$t\bar{t} \to \mu + \text{jets}$	3.8±0.1	$60.3\ ^{+2.8}_{-2.7}$	7.7±0.2	$59.0\ ^{+2.8}_{-2.7}$
$t\bar{t} \to l^+l^- + \text{jets}$	43.7±0.4	$60.2\ ^{+2.8}_{-2.7}$	20.6±0.3	$61.4\ ^{+2.9}_{-2.8}$

TABLE III: Expected event yields in the two analysis channels assuming the measured $t\bar{t}$ production cross section of 6.9 pb.

	Tau-type 1 and 2	Tau-type 3
$t\bar{t} \to \tau_h + \text{jets}$	27.60±5.25	22.11±4.70
$t\bar{t} \to e + \text{jets}$	26.25±5.12	5.94±2.44
$t\bar{t} \to \mu + \text{jets}$	1.95±1.40	3.68±1.92
$t\bar{t} \to l^+l^- + \text{jets}$	5.52±2.35	2.69±1.64
Total $t\bar{t} \to$ leptons	61.32±7.83	34.42±5.87
W+jets	13.48±3.67	6.01±2.45
Z+jets	3.35±1.83	1.96±1.40

$1083.2^{+11.3}_{-10.3}$ (stat), for the two channels, respectively. The numbers of $t\bar{t}$ events are comparable to the expected values given in Table III.

To minimize the statistical uncertainty of the measurement of $\sigma(p\bar{p} \to t\bar{t} + X) \cdot \text{BR}(t\bar{t} \to \tau_h + \text{jets})$, which we denote as $\sigma_{t\bar{t}} \cdot \text{BR}_{\tau_h+j}$, we fit the entire NN_{sb} output distribution rather than counting events above a given value. The value of $\sigma_{t\bar{t}} \cdot \text{BR}_{\tau_h+j}$ and the fraction of multijet background in the sample are obtained from a negative log-likelihood fit to the NN_{sb} distributions for tau-types 1 and 2 and tau-type 3, independently:

$$L(\sigma_{t\bar{t}}, \tilde{N}_i, N_i^{\text{obs}}) = -\log\left(\prod_i \frac{\tilde{N}_i^{N_i^{\text{obs}}}}{N_i^{\text{obs}}!} e^{-\tilde{N}_i}\right), \quad (1)$$

where $\tilde{N}_i = \sigma_{t\bar{t}} \times \sum_j \epsilon^i_{t\bar{t}(j)} \times \text{BR}_{t\bar{t}(j)} \times \mathcal{L} + N_{\text{bkg},i}$ is the expected number of events in the i^{th} bin of the NN_{sb} histogram for a given $\sigma_{t\bar{t}}$, with integrated luminosity $\mathcal{L}$, number of background events $N_{\text{bkg},i}$, and the efficiency (BR) for the j^{th} $t\bar{t}$ leptonic channel $\epsilon_{t\bar{t}(j)}$ ($\text{BR}_{t\bar{t}(j)}$), and N_i^{obs} is the observed number of events in the i^{th} bin.

The measured value of $\sigma_{t\bar{t}} \cdot \text{BR}_{\tau_h+j}$ is

$$0.60^{+0.23}_{-0.22}\ (\text{stat})\ ^{+0.15}_{-0.14}\ (\text{syst}) \pm 0.04\ (\text{lumi})\ \text{pb},$$

where we combine the tau-type 1 and 2 measurement with the tau-type 3 measurement. Using the theoretical cross section $\sigma_{t\bar{t}} = 8.06^{+0.52}_{-0.73}$ pb for $m_t = 170$ GeV from Ref. [5], we measure $\text{BR}_{\tau_h+j} = 0.074^{+0.029}_{-0.027}$ which is consistent with the SM value given in Table I.

Table IV summarizes the systematic uncertainties on $\sigma_{t\bar{t}} \cdot \text{BR}_{\tau_h+j}$. These are calculated by varying the source by plus and minus one standard deviation, and propagating the uncertainty to the final $\sigma_{t\bar{t}} \cdot \text{BR}_{\tau_h+j}$. The jet energy corrections account for the effect of the jet energy scale and resolution. Jet identification takes account of the difference in the jet finding efficiency in data and MC. The b-tagging entry accounts for the systematic uncertainties on its efficiency. The τ lepton identification uncertainty is derived by fluctuating the value of each input variable within its statistical uncertainty and observing its effect on the NN_τ output. The trigger category accounts for the uncertainty in the multijet trigger turn-on and also takes into account the possibility that a multijet event with a τ lepton can have a different trigger turn-on. Multijet modeling accounts for the uncertainty of the multijet sample to model the $t\bar{t} \to \tau_h + \text{jets}$ background and its limited statistics. The category $W + \text{jets}$ modeling accounts for the uncertainty in the scale factor both for light flavor jets and heavy flavor jets, and the uncertainty in the PDF. The $t\bar{t}$ cross section systematic uncertainty represents the effect of the normalization of the non-tau lepton $t\bar{t}$ background, which is normalized to the theoretical value of the cross section. In addition to the sources listed in Table IV, there is a ±6.1% uncertainty in the luminosity measurement [28].

In addition, we present the combined measurement of the production cross section for $t\bar{t}$ using all measured $t\bar{t}$ channels with leptons in the final state listed in Table III that satisfy the selection criteria described above. We repeat the negative log-likelihood fit for the number of $t\bar{t}$ signal and multijet background events fixing the $t\bar{t}$ BRs to their SM values, but this time fit for all $t\bar{t}$ channels arriving at 60.5 ± 11.8 (stat) events and 24.0 ± 11.4 (stat) events for channels with tau-types 1 and 2 and with tau-type 3 characteristics, respectively. The fitted multijet backgrounds in this case are 336.7 ± 11.8 (stat) events and 1083.2 ± 11.4 (stat) events, for the two channels, respectively. The production cross section is calculated using the negative log-likelihood defined in Eq. 1 for tau-types 1 and 2 and tau-type 3 separately. The two cross sections are then combined to give

$$\sigma_{t\bar{t}} = 6.9\ ^{+1.2}_{-1.2}\ (\text{stat})\ ^{+0.8}_{-0.7}\ (\text{syst}) \pm 0.4\ (\text{lumi})\ \text{pb}.$$

To estimate the dependence on m_t, we repeat the mea-

TABLE IV: Systematic uncertainties on $\sigma_{t\bar{t}} \cdot \mathrm{BR}_{\tau_h+j}$ (in pb) as measured for the $t\bar{t} \to \tau_h +$ jets channel.

Source	τ_h+jets (types 1 and 2)		τ_h+jets (type 3)		Combined	
Jet energy corrections	-0.078	$+0.081$	-0.047	$+0.047$	-0.068	$+0.069$
Jet identification	-0.019	$+0.019$	-0.012	$+0.012$	-0.016	$+0.016$
b tagging	-0.074	$+0.084$	-0.035	$+0.041$	-0.060	$+0.068$
Tau identification	-0.035	$+0.035$	-0.020	$+0.021$	-0.029	$+0.029$
Trigger	-0.002	$+0.053$	-0.000	$+0.027$	-0.002	$+0.043$
Multijet modeling	-0.090	$+0.090$	-0.169	$+0.169$	-0.083	$+0.083$
$W +$ jets modeling	-0.028	$+0.028$	-0.012	$+0.013$	-0.023	$+0.022$
$t\bar{t}$ cross section	-0.064	$+0.068$	-0.029	$+0.030$	-0.052	$+0.055$
Total systematic uncertainty	-0.16	$+0.15$	-0.18	$+0.15$	-0.14	$+0.15$

surement using $m_t = 175$ GeV and find

$$\sigma_{t\bar{t}} = 6.3\ ^{+1.2}_{-1.1}\ (\mathrm{stat})\ \pm^{+0.7}_{-0.7}\ (\mathrm{syst}) \pm 0.4\ (\mathrm{lumi})\ \mathrm{pb}.$$

In summary, we have performed a measurement of $\sigma_{t\bar{t}} \cdot \mathrm{BR}_{\tau_h+j} = 0.60^{+0.28}_{-0.26}$ pb and, using the theoretical $t\bar{t}$ production cross section, extracted $\mathrm{BR}_{\tau_h+j} = 0.074^{+0.029}_{-0.027}$, which agrees with the SM expectation. In addition, we have performed a measurement of the $p\bar{p} \to t\bar{t} + X$ production cross section, $\sigma_{t\bar{t}} = 6.9\ ^{+1.5}_{-1.4}$ pb, using the $t\bar{t} \to \tau_h +$ jets topology. The measurement is in agreement with the SM [3–5] and previous experimental measurements using other $t\bar{t}$ channels [18] at the Tevatron.

We thank the staffs at Fermilab and collaborating institutions, and acknowledge support from the DOE and NSF (USA); CEA and CNRS/IN2P3 (France); FASI, Rosatom and RFBR (Russia); CNPq, FAPERJ, FAPESP and FUNDUNESP (Brazil); DAE and DST (India); Colciencias (Colombia); CONACyT (Mexico); KRF and KOSEF (Korea); CONICET and UBACyT (Argentina); FOM (The Netherlands); STFC and the Royal Society (United Kingdom); MSMT and GACR (Czech Republic); CRC Program and NSERC (Canada); BMBF and DFG (Germany); SFI (Ireland); The Swedish Research Council (Sweden); and CAS and CNSF (China).

[1] V. Barger and R.J.N. Phillips, Phys. Rev. D **41**, 884 (1990).
[2] J. Guasch and J. Sola, Phys. Lett. B **416**, 353 (1998).
[3] M. Cacciari *et al.*, J. High Energy Phys. **09**, 127 (2008).
[4] N. Kidonakis and R. Vogt, Phys. Rev. D **78**, 074005 (2008).
[5] S. Moch and P. Uwer, Phys. Rev. D **78**, 034003 (2008).
[6] T. Han and M.B. Magro, Phys. Lett. B **476**, 79 (2000).
[7] C. Yue, H. Zong and L. Liu, Mod. Phys. Lett. **74**, 2626, (2003).
[8] V.M. Abazov *et al.* (D0 Collaboration), Nucl. Instrum. Methods Phys. Res. A **565**, 463 (2006).
[9] V.M. Abazov *et al.* (D0 Collaboration), Phys. Lett. B **679**, 177 (2009).
[10] A. Abulencia *et al.* (CDF Collaboration), Phys. Lett. B **639**, 172 (2006).
[11] V.M. Abazov *et al.* (D0 Collaboration), Phys. Rev. D **82**, 032002 (2010).
[12] A. Schwartzman, Report No. FERMILAB-THESIS-2004-2.
[13] G.C. Blazey *et al.*, in *Proceedings of the Workshop: QCD and Weak Boson Physics in Run II,* edited by U. Baur, R.K. Ellis, and D. Zeppenfeld, Fermilab-Pub-00/297 (2000).
[14] The D0 coordinate system has the positive z-axis along the proton beamline, and $z = 0$ at the center of the detector. The polar and azimuthal angles are denoted as θ and ϕ, respectively. The pseudorapidity is defined as $\eta = -\ln(\tan\frac{\theta}{2})$.
[15] J. Hegeman, J. Phys. Conf. Ser. **160**, 012024 (2009).
[16] V.M. Abazov *et al.* (D0 Collaboration), Phys. Lett. B **670**, 292 (2009).
[17] V.M. Abazov *et al.* (D0 Collaboration), Phys. Rev. D **76**, 092007 (2007).
[18] C. Amsler *et al.* (Particle Data Group), Phys. Lett. B **667**, 1 (2008).
[19] M.L. Mangano *et al.*, J. High Energy Phys. **07**, 001 (2003).
[20] J. Pumplin *et al.*, J. High Energy Phys. **07**, 012 (2002); D. Stump *et al.*, J. High Energy Phys. **10**, 046 (2003).
[21] T. Sjöstrand *et al.*, Comput. Phys. Commun. **135**, 238 (2001).
[22] D.J. Lange, Nucl. Instrum. Methods Phys. Res. A **462**, 152 (2001).
[23] S. Jadach, Z. Was, R. Decker, and J.H. Kuehn, Comp. Phys. Commun. **76**, 361 (1993).
[24] S. Höche *et al.*, arXiv:hep-ph/0602031 (2004).
[25] R. Brun and F. Carminati, CERN Program Library Long Writeup W5013 (unpublished), (1993).
[26] V.M. Abazov *et al.* (D0 Collaboration), Nucl. Instr. and Methods Phys. Res. A **620**, 490 (2010).
[27] The aplanarity is $3/2\lambda_3$, with λ_3 being the smallest eigenvalue of the momentum tensor $M^{\alpha\beta} = \sum_i p_i^\alpha p_i^\beta / \sum_i |\vec{p}_i|^2$, where i runs over the number of jets and the τ lepton candidate, and $\alpha, \beta = 1, 2, 3$ specifies the three spatial components of the momentum.
[28] T. Andeen *et al.*, FERMILAB-TM-2365 (2007).